Published in final edited form as:
J Mol Recognit. 2012 April ; 25(4): 216–223. doi:10.1002/jmr.2174.

Classifying compound mechanism of action for linking whole cell phenotypes to molecular targets

Christina R. Bourne[1,*], **Nancy Wakeham**[1], **Richard A. Bunce**[2], **K. Darrell Berlin**[2], and **William W. Barrow**[1,*]

[1]Department of Veterinary Pathobiology, Oklahoma State University, 250 McElroy Hall, Stillwater OK 74078

[2]Department of Chemistry, Oklahoma State University, 107 Physical Sciences 1, Stillwater OK 74078

Abstract

Drug development programs have proven successful when performed at a whole cell level, thus incorporating solubility and permeability into the primary screen. However, linking those results to the target within the cell has been a major set-back. The Phenotype Microarray system, marketed and sold by Biolog, seeks to address this need by assessing the phenotype in combination with a variety of chemicals with known mechanism of action (MOA). We have evaluated this system for usefulness in deducing the MOA for three test compounds. To achieve this, we constructed a database with 21 known antimicrobials, which served as a comparison for grouping our unknown MOA compounds. Pearson correlation and Ward linkage calculations were used to generate a dendrogram that produced clustering largely by known MOA, although there were exceptions. Of the three unknown compounds, one was definitively placed as an anti-folate. The second and third compounds' MOA were not clearly identified, likely due to unique MOA not represented within the commercial database. The availability of the database generated in this report for *S. aureus* ATCC 29213 will increase the accessibility of this technique to other investigators. From our analysis, the Phenotype Microarray system can group compounds with clear MOA, but distinction of unique or broadly acting MOA at this time is less clear.

Keywords

mechanism of action; Phenotype Microarray; antimicrobial; phenotype; molecular target; anti-folate; dendrogram; isobologram

INTRODUCTION

High throughput drug discovery efforts have followed two parallel paths: target based pathway screening and whole cell phenotypic screening. The advent of sequences of whole genomes was believed an advantage toward target-based assays by identifying non-redundant or essential targets (Mills 2006). The fruit of more than a decade of focused effort at target screening did not deliver usable therapeutics (Payne, Gwynn et al. 2007). Screening for a whole cell phenotype has the advantage of incorporating cell permeability and solubility in the primary screen, but suffers from a lack of knowledge of specific targets, and

[*]**Corresponding authors:** Mailing address: Department of Veterinary Pathobiology, Oklahoma State University, 250 McElroy Hall, Stillwater OK, 74078. Contact for C.R. Bourne: christina.bourne@okstate.edu 405-744-6736 (phone) 405-744-5275 (fax). Contact for W.W. Barrow: bill.barrow@okstate.edu 405-744-1842 (phone) 405-744-3738 (fax).

translating hits from these experiments into a defined mechanism of action (MOA) is laborious (Baker 2010; Fulmer 2011).

Experimental methods to address the identification of an unknown target from a phenotypic screen have been developed; however, these approaches require high overhead for set-up of experimental systems, and they have limited portability between bacterial strains. Some examples include experiments with transposon mutagenesis or related methods of reverse chemical genetics to identify targets of small molecules (Miller, Bundy et al. 2008). This idea was further developed with applications of gene signatures and RNAi methods, such as Elitra Pharmaceuticals *S. aureus* TargetArray (Brazas and Hancock 2005; Xu, Trawick et al. 2010). Recent studies have advanced to forward chemical genetics, also termed multi-copy suppression (Li, Zolli-Juran et al. 2004; Stirrett, Ferreras et al. 2008; Wang, Claveau et al. 2011). Some *in silico* methods have identified targets based on compound activity profiling using “guilt-by-association” algorithms (Plouffe, Brinker et al. 2008), as well as mining of chemical databases such as ChEMBL (Gaulton, Bellis et al. 2011). While the Phenotype Microarray system does not deliver a single target, it has an advantage in minimal set-up once a database set is generated, and experiments can then be completed in a few days.

We have undertaken the Phenoype Microarray (PM) system from Biolog in efforts to extend information for growth inhibitors identified from primary whole cell screens (Bochner 2003; Barrow, Dreier et al. 2007; Biolog Application Notes). The PM system employs two parts: ten 96-well plates to evaluate metabolic usage and another ten 96-well plates to assess chemical sensitivities to known antibacterials, microbicides, toxic ions and detergents. The ten plate metabolomic component of this screening technology, not utilized in the current report, has been readily applied to the studies of different bacterial strains, unique properties of halophiles, mutants in pathways of interest, and to hunt for gain of function related to pathogenesis for use as drug targets (Tracy, Edwards et al. 2002; dela Cruz, Schulz et al. 2006; Loh, Gyaneshwar et al. 2006; Seidl, Druzhinina et al. 2006; Nagy, Seidl et al. 2007; Tohsato and Mori 2008; Zhang and Rainey 2008; Edwards, Dalebroux et al. 2009; Sabet, Diallo et al. 2009; Fabich, Leatham et al. 2011). Applications using the chemical sensitivity plates seem to be continually developing. Reports have been published using the chemical sensitivity technology to analyze components of pathways as well as antibiotic resistance phenotypes in greater detail (Sauer, Bachman et al. 2005; von Eiff, McNamara et al. 2006; Bailey, Paulsen et al. 2008; Mesak and Davies 2009; Pietiainen, Francois et al. 2009; Tremaroli, Workentine et al. 2009; Zhang and Biswas 2009). However, the major role for this system as presented by Biolog is for use in drug development by inference of the MOA of a given compound; experimental applications of this approach are missing from the literature.

To initiate this investigation we have constructed a database of 21 commercial antimicrobial compounds to serve as a comparative database. Compounds were chosen to maximize representatives of MOA while attempting to minimize the number of compounds. Further, each compound needed to be effective against our test organism, *S. aureus* ATCC 29213. As the Biolog system uses different media and growth conditions from conventional Clinical and Laboratory Standards Institute (CLSI) methods (CLSI 2009), minimum inhibitory concentration (MIC) values were determined with both CLSI and Phenotype Microarray reagents. We used this database to infer the MOA for three compounds under development. One of these has already been identified as an inhibitor of dihydrofolate reductase (DHFR) (Bourne, Barrow et al. 2010); the other two compounds were identified by a medium-throughput whole cell screen for inhibitors of bacterial growth (Barrow, Bourne et al. 2007). While these two compounds have unknown MOA, some prior information has been gathered using the compounds’ structure in literature and database searches.

We found the PM chemical sensitivity assay was able to group similar MOA compounds in most cases, but experiments had to be performed at very similar sub-MIC concentrations between all compounds. In addition, data processing methods had to be developed and mechanisms were derived to deal with inherent noise within the system while maintaining the diversity of response to yield valid groupings with a minimum number of samples. The MOA of the anti-folate RAB1 was confirmed by these studies, while limited insights were gained into the MOA of the other two test compounds.

MATERIALS & METHODS

Commercial antimicrobial compounds

All compounds were purchased from Sigma unless noted. Abbreviations are as specified in CLSI documents (CLSI 2010): GEN, gentamicin; TOB, tobramycin; DOX, doxycycline; TET, tetracycline; CLI, clindamycin; CHL, chloramphenicol; ERY, erythromycin; LNZ, linezolid; IPM, imipenem; MEM, meropenem; CTX, cefotaxime; CFX, cefuroxime; OXA, oxacillin; PEN, penicillin G; VAN, vancomycin; DAP, daptomycin; CIP, ciprofloxacin (Mediatech, Inc.); LEV, levofloxacin; TMP, trimethoprim; SXT, 1 part trimethoprim to 19 parts sulfamethoxazole; RIF, rifampin. RAB1 was synthesized as described previously (Bourne, Bunce et al. 2009); 6628 and 6021 were purchased from Sigma Aldrich.

Determination of minimum inhibitory concentration (MIC)

MIC determinations followed the CLSI recommended guidelines for the broth microdilution method or were carried out as below for the PM assays (CLSI 2009). Major differences between the two MIC methods were (1) *S. aureus* ATCC 29213 was propagated on trypticase-soy agar for the CLSI method, or on Biolog Universal Growth with 5% sheep's blood (BUG-B) for the Biolog method, (2) inoculating fluids were saline/CAMBH for the CLSI method, and were IF-0a/IF-10b for the Biolog method, (3) incubation temperature was 37 °C and time was 18 – 20 hours for the CLSI method, and was 33 °C for 24 hours for the Biolog method, (4) CLSI MIC values were determined using the turbidity of growth at 600nm, while for the Biolog method the MIC cutoffs were determined based on colorimetric changes in Redox Dye H, (5) the colony forming unit for inoculation using the CLSI method was in the range of $2 – 8 \times 10^5$, while for the Biolog method it was $2 – 4 \times 10^6$.

Phenotype Microarray (PM) assays

Each antimicrobial or test compound was tested within a single run, which consisted of a control set of ten plates with only vehicle (referred to as the "plus zero" set), a set with 0.1× MIC, a set with 0.25× MIC, and a set with 0.5× MIC, where MIC is determined using Biolog reagents, and resulting in forty 96-well plates per assay. Each plate contains 24 different chemicals dried in the wells, each at four concentrations ("plated compounds"). Respiration of the bacteria was detected by colorimetric reaction with Biolog's tetrazolium based Redox Dye H (Bochner 2003). Color changes were recorded by an Omnilog system at 15-minute intervals for 48 hours at 33 °C. Reagents and experimental procedures followed the recommended protocol from Biolog. Inocula were prepared in Biolog's 1.2× IF-0a fluid using a turbidimeter to adjust the cell density to 85% relative to an 85% Turbidity standard (Biolog). The inocula were diluted ten-fold into Biolog 1× IF-10b fluid containing 1% Redox Dye H and the appropriate concentration of antimicrobial or test compound, diluted from stock solutions of either water or dimethylsulfoxide (DMSO), as solubility allowed; 100uL was delivered to each well. Electronic files were captured from the Omnilog system computer, converted with Biolog's Data File Converter utility, partitioned into sets with their File Management software, and parameters of the growth curves exported with their Parametric software (version 1.20.02).

Calculation of Phenotype Microarray assay results

Raw numbers for the "height" parameter, defined as "the average height of the plot" (in arbitrary units corresponding to color changes upon bacterial respiration) were imported into Excel, arranged by Biolog plate, well number for plated compounds (1 – 4), and finally by ×MIC for each tested compound (these are available for each commercial antimicrobial as part of the Supporting Information). To enhance the interpretability of the isobolograms, raw numbers were converted to a percent growth using the following formula (Wiater, Madejska et al. 2007): % growth = [log(Height, data point) − log(Height, minimum)] / [log(Height, maximum in plate) − log(Height, minimum)]. These values were used to construct isobolograms within Excel as 3D contour plots (raw data and spreadsheets suitable for calculations with new raw data are available in the Supporting Material).

Processing attempted to maintain the rationale that Biolog had previously used (Wiater, Madejska et al. 2007), but calculations were formulated to reflect the difference in growth upon titration of plated compounds (wells 1 – 4) and the added compounds (0×, 0.1×, 0.25× and 0.5× MIC) in efforts to capture the resulting shape of the isobologram. To this end, data composing an isobologram were partitioned into discrete blocks along each axis and an equation for finding the area of an irregular polygon (surveyor's area) was applied (Braden 1986). For the plated compounds, the area was calculated for each well from the × MIC values and the % growth; for the added compounds, the area was calculated for each × MIC value from the well number (1 – 4) and the % growth.

These calculations yielded a series of four area values for the concentrations of plated compound and four for the concentrations of added compound across the isobologram. To capture the change in area, successive area measurements were subtracted from the previous value such that the more dilute concentration was subtracted from a higher concentration, giving a series of delta (area), or d(A), for each isobologram axis. If this number was positive, it indicated an increase of growth as the compound concentration increased, suggesting a growth enhancing effect. If this number was negative, it indicated a decrease in growth as the compound concentration increased, indicative of some level of inhibition.

The d(A) for each isobologram axis, one calculated from the plated-compounds and the other calculated from the added compounds, were then summed to yield a final single numeric parameter representative of: (1) the four concentrations of the plated compound and (2) the three concentrations (and the "plus zero" control) of test compound. These values were normalized per data set by converting to fractional values, yielding a maximum of 1.0 (maximum increase in growth as the concentrations increased) and a minimum of 0 (maximum decrease in growth as the concentrations increased).

The agreement of the raw "height" signal was assessed with the independent control "plus zero" sets for each of the 21 antimicrobials. Raw data points that displayed a standard deviation greater than 20% for any of the four plated compound concentrations were excluded from further calculations, as these were deemed to be inherently noisy independent of any added compound (Supporting Material Table 1).

After removal of data points with inherent variation, the remaining data set was enriched for variation arising from the added compounds by including only points that exceeded 10% standard deviation (enriched data included in Supporting Material Figure 1). Inclusion of data with limited variation (< 10%) diluted the relationship between compounds and resulted in shallow linkage distances, although the pattern of clustering was maintained (data not shown). Processing continued following Biolog's procedure by applying a linkage analysis based on Pearson distance calculations to determine the similarity of each antimicrobial or test compound to the other, as well as a one-sided significance value (Figure 1) (Wiater,

Madejska et al. 2007). The result is a table of correlation values, which is then used to produce a final dendrogram with the most similar responses grouped together (Figure 2). Combinations with $p > 0.05$ were excluded from the clustering, which used a Ward hierarchical analysis; Pearson correlation and Ward clustering were carried out with the excel add-on winSTAT. (product of R. Fitch, www.winstat.com).

RESULTS & DISCUSSION

Different MIC values arising from different methodologies

The MIC was determined using the same methodology as the Biolog experiments, as the composition of the media, incubation temperature, growth time and inocula composition are different. In addition, the Biolog protocol utilizes a colorimetric redox-sensitive dye to indicate growth. MIC determinations were also performed in-house using standardized CLSI conditions to ensure reproducibility for comparisons. In all cases the CLSI conditions yielded the same MIC values as previously published, although some, such as the aminoglycosides GEN and TOB, were more defined with in-house measurements (Table 1, CLSI reported 0.12–1 μg/mL, while in-house experiments yielded 0.25–0.5 μg/mL) (CLSI 2010). However, in some instances the MIC determination carried out with Biolog reagents yielded a higher value than CLSI methods, such as the aforementioned GEN and TOB, which were elevated to 2 μg/mL with Biolog methods. A likely explanation is the incubation temperature and time, which for CLSI is 37 °C for 18–20 hours and for Biolog is 33 °C for 24 hours (Wiater, Madejska et al. 2007; CLSI 2009). In addition, the colorimetric reagent is likely more sensitive to bacterial respiration, while CLSI methods rely on active growth to produce turbidity within the solution (Bochner, Siri et al. 2011).

There were two antimicrobials that gave particularly increased MIC values with Biolog reagents. The MIC for PEN, a beta-lactam antibiotic that inhibits peptidoglycan cross-linking (Yocum, Rasmussen et al. 1980), increased from 1 μg/mL with CLSI methods to 32 μg/mL with Biolog reagents. This did not occur with the other representative from the penicillin class (OXA), or other beta-lactam antibiotics (CTX, CFX). The other example of an elevated MIC is daptomycin, a lipopeptide antibiotic with a unique MOA that causes rapid membrane depolarization (Ho, Jung et al. 2008; Robbel and Marahiel 2010). The MIC for DAP increased from 1–4 μg/mL (including addition of $CaCl_2$ at 50 μg/mL) with the CLSI method up to 50 μg/mL with Biolog reagents. This dramatic increase is likely due to interference from cations other than calcium in the media, as this has been noted to increase the MIC by up to 32-fold in other systems (Ho, Jung et al. 2008).

Calculation of PM assay results

As each compound was analyzed with a negative control plate set, these “plus zero” controls served as a way to assess the inherent variable response of this system irrespective of the added compounds. The raw data signal for each individual well was compared for all 21 “plus zero” data sets, and points were flagged for removal if any exceeded 20% of the standard deviation from the average, an empirically determined cut-off level. As each of the 240 plated compounds are present at four concentrations, excessive variation at any of the four concentrations was considered grounds for removal of that plated compound from the analysis. This resulted in the exclusion of 49 plated compounds (Supporting Material Table 1). Among those culled, sodium cyanide, a general respiration disruptor, had excessive variation at all four plated concentrations. Amikacin (an aminoglycoside), dodine & guanidine hydrochloride (non-specific membrane chaotropes), dichlofluanid (phenylsulphamide, used as an antifungal), methyltrioctylammonium chloride (non-specific membrane detergent), and 5,7-dichloro-8-hydroxy-quinaldine (lipophilic chelator) all displayed excessive variation in three of the four plated concentrations.

The remaining 196 values for plated compounds per data set were enriched for variation due to the added compound. This was achieved by selecting only points with > 10% standard deviation between all data sets, resulting in 164 plated compounds analyzed from the original 240. The rationale behind this action was that plated compounds that behave the same with every tested antimicrobial or test compound would strengthen agreement regardless of MOA, thus diluting the effective variation useful to class assignment. The drawback to this approach is that it must be repeated with the addition of any new data set, possibly creating some variation with each new analysis, although in practice only two to five data points were affected by this re-calculation.

Pearson correlations were used to assess the linear pairwise dependence of each data set's deviation from random noise, such that the more similar the data sets the closer the correlation value approaches 1 (Figure 1). This analysis also generated a one-sided significance that was used to remove data sets with a low probability ($p > 0.05$) of significance (indicated by grey boxes in Figure 1). An indicator of the reliability of this type of correlation due to sample size is Cronbach's alpha, which was excellent at 0.95; further, the homogeneity-quotient, which indicates the level of variability, was 0.44. It was noted in these analyses that values of the homogeneity-coefficient greater than ~ 0.6, as was obtained before enriching with variability > 10% standard deviation, resulted in shallow clustering.

Clustering Results for Commercial Antimicrobials

The clustering results for the generated database were successful despite the relatively limited number of members per MOA, as well as including only 3 concentrations of antimicrobial or test compound (Figure 2). Two major divisions arose among 21 commercial antimicrobials and three test compounds. This grouped the folate pathway inhibitors TMP, SXT and RAB1 into one tight cluster, and GEN, VAN, TOB within another tight cluster within the first division. These groupings are easy to visualize in the correlations (Figure 1) and the data (Supporting Material Table 2), as the folate pathway inhibitors display a strong decrease in growth in combination with plated sulfa compounds. Among anti-folates a strong synergy is known when administered with sulfa drugs such as sulfamethoxazole (SXT for *in vitro* testing is 1 part TMP to 19 parts sulfamethoxazole) (Grim, Rapp et al. 2005). The same phenotype is observed with GEN, VAN, TOB, which is unexpected. However, the data for GEN, VAN, TOB compounds display more deviations as compared to all other compounds, and it is unclear what significance their individual responses may have. These three compounds, particularly VAN, seem to favor greater growth inhibition than all other compounds (Supporting Material Table 2, smaller numbers, shaded blue). In addition, GEN, VAN, TOB are the only compounds to display poor significance in correlation values (Figure 1, grey boxes).

The other major division contains the remaining 18 compounds analyzed in these experiments (Figure 2). These 18 compounds are distributed into five clear branches, with some further hierarchy among individuals. Inhibitors of protein synthesis that group together are DOX (tetracycline), LNZ (synthesis), ERY (macrolide), CLI (lincosamide), which are interestingly also grouped with the cell wall acting beta-lactam inhibitor PEN (penicillin). This grouping is most closely correlated to the two compounds with unknown MOA, 6628 and 6021. These two clusters are most closely correlated to a group of inhibitors acting on the bacterial cell wall, encompassing IPM (carbepenem), CFX (cephem), MEM (carbepenem), OXA (penicillin) and CTX (cephem).

This second major division is completed by two branches, one composed of TET (tetracycline), DAP (membrane depolarization), CHL (50S ribosome inhibitor), and the other composed of CIP (quinolone), LEV (quinolone), RIF (RNA polymerase). It is reasonable that the quinolones, which interfere with DNA unwinding, would group with the

RNA polymerase inhibitor RIF, as RNA polymerase would need to read through the uncoiled DNA to perform its cellular function.

The clustering of TET and CHL apart from other inhibitors involved in steps of protein synthesis results from subtle differences. These differences result from a more enhanced growth, largely in response to some sulfa compounds, nitro-containing and oxidizing compounds, aminoglycosides, and cephalosporins (Supporting Material Figure 1). It is not clear why this is, but it is apparent from inspection of the correlation values that while there appears to be some cross-correlation among all protein synthesis inhibitors, it isn't strong enough to impact the final clustering (Figure 2). In such cases, it is useful to envision MOA as a spectrum of primary and secondary effects. Further, a known MOA does not indicate full exploitation of the compound's abilities, particularly at sub-MIC concentrations as tested in the current assays, and this may be affecting the responses of TET and CHL such that they appear more similar to DAP than to other protein synthesis inhibitors.

Clustering of test compounds using the database of commercial antimicrobials

As part of our investigations we tested three compounds that were not commercially available antimicrobials. Among these, RAB1 has a known MOA and belongs to a class of anti-folates that inhibits dihydrofolate reductase (Bourne, Barrow et al. 2010). The clustering of RAB1 with known anti-folates TMP and SXT provides a validation of this method, both for experimental parameters and calculation procedures. RAB1 and TMP have a weak correlation with quinolones (range 0.54 – 0.59, Figure 1), but are not closely correlated with any other compounds. For SXT, the closest correlation outside of the anti-folate cluster is to 6628 (0.53), although 6628 has much higher correlations with other compounds (Figure 1).

The compounds identified as 6628 and 6021 were selected based on the screening of whole cell phenotypes (Barrow, Bourne et al. 2007). These compounds were identified as having an MIC ≤ 16 μg/mL against at least one of the tested bacterial agents (*B. anthracis*, *Y. pestis*, *B. abortus* or *F. tularensis*, unpublished data). When the structures of these compounds were examined, 6628 was noted to contain a sulfonamide moiety similar to other sulfa-drugs that target DHPS (Skold 2000), while 6021 was found in the PubChem BioAssay database (National Center for Biotechnology Information AID=372) to be a known inhibitor of HIV1 RNaseH1 (Figure 3).

The current study was unable to cluster either 6628 or 6021 with compounds of known MOA. Among anti-folates, TMP and RAB1 inhibit the DHFR enzyme, and a decreased growth is noted when also treated with sulfa drugs (Supporting Material Table 2). However, there is no appreciable effect when TMP or RAB1 are added to wells already containing TMP. This is in contrast to SXT, which showed decreased growth in the presence of plated sulfa-compounds as well as TMP. 6628 showed modest growth reduction with sulfa-compounds and no appreciable effect on growth with plated TMP.

We have attempted to evaluate the anti-folate capacity of 6628 using recombinant DHPS from *B. anthracis*, which had an MIC of 4 μg/mL for 6628, although this DHPS is naturally resistant to many sulfonamides (Valderas, Andi et al. 2008). Using the PiPer Pyrophosphate Assay (Invitrogen) DHPS yielded only a weak signal above background, and no inhibition with 6628 or related series compounds were identified (data not shown). This is consistent with a published report finding the antimicrobial activity of benzene-sulfonamides was not dependent on the amide region, leading to a conclusion that they are not acting as traditional sulfonamides (Namba, Zheng et al. 2008). Structural similarities to 6628 have been noted for inhibitors of human 5-aminoimidazole-4-carboxamide ribonucleotide transformylase (AICAR) (Cheong, Wolan et al. 2004; Li, Xu et al. 2004; Xu, Li et al. 2004), human

methionine aminopeptidase type II (Kawai, BaMaung et al. 2006), and to sulfasalazine, which was shown to inhibit human sepiapterin reductase (Chidley, Haruki et al. 2011) (Figure 3). In each case no information is available about the potential role of these enzymes as antimicrobial targets. It would be interesting to extend the current database to include these inhibitors, and to evaluate the response in comparison to that of 6628.

Compound 6021 was identified in the PubChem BioAssay database as an anti-viral that targets the RNaseH domain of HIV1 and 2 (National Center for Biotechnology Information AID=372), as well as E. coli (National Center for Biotechnology Information AID=365) and human RNase H1 (National Center for Biotechnology Information AID=366). RNaseH1 is essential in bacteria as it digests RNA from a DNA:RNA hybrid, such as found in Okazaki fragments during replication (Tadokoro and Kanaya 2009). Compound 6021 clusters with 6628, and these are most closely correlated with inhibitors of protein synthesis (DOX, LNZ, ERY, PEN, CLI). However, examination of the correlation values (Figure 1) reveal that neither 6628 nor 6021 are particularly well correlated with any other MOA; the highest non-self values for 6628 are 0.6 with LNZ and LEV, and for 6021 are 0.59 with ERY and 0.56 with PEN. Examination of the response data expressed as d(A) does not delineate a clear pattern for either compound (Supporting Material Table 2).

While there were no clear predictions for the clustering result based on 6021's putative MOA, it was unexpected to partition with compounds targeting protein production. The putative MOA was considered most likely to be similar to inhibitors of DNA replication. It is possible that bacterial RNaseH1 plays unappreciated roles in cellular maintenance. 6021's inhibitory activity may also arise due to similarity to an RNA nucleotide (Figure 3, adenine is shown as an example). As with 6628, it would be interesting to evaluate the responses of other RNaseH1 inhibitors as tallied in the BioAssay repository for comparison to 6021. We have demonstrated direct inhibition of bacterial RNaseH1 proteins by 6021, and shown species variation in this inhibitory activity (data not shown), arguing for a specific rather than generic target. For both 6628 and 6021 this may be a case of a unique target, which is unable to cluster successfully with known antimicrobials.

CONCLUSIONS

The Phenotype Microarray assay system is marketed for determining compound MOA (Biolog Application Notes). From the current investigation, this system can correctly assign MOA, as for commercial antimicrobials and for RAB1. Clustering results were not particularly fine, in that the identified MOA was broad in nature and could not distinguish specifics of the targets, such as tetracyclines versus macrolides. However, aminoglycosides did partition together and away from all other protein synthesis inhibitors. We did not note any effect of bactericidal versus bacteriostatic in these experiments. In the case of 6628 and 6021 there are no clear MOA from these analyses; this may be due to their unique MOA. It is likely that application of the PM system to unique MOA will only be possible by first deducing putative MOA followed by seeding the comparator database with similar MOA compounds, even if they are not commercial antimicrobials. The current investigations highlighted the importance of determining the MIC using the same solutions and conditions as the PM assay, as in the case of DAP. We also found a subtle effect from changing the sub MIC concentrations of test compounds, which seemed to alter the clustering (data not shown), leading to the adoption of standardized concentrations among all database members.

The major deviation from marketed purpose noted in these analyses is the inability to assign synergy or antagonism, which was the cornerstone of the calculation method as presented by Biolog (Wiater, Madejska et al. 2007). The assignment of synergy or antagonism is a useful descriptor, but can only be calculated with knowledge of the MIC for all compounds in the

combination (Lorian 1996; Chou 2010; Peifer, Weiss et al. 2010; Brunton, Chabner et al. 2011); in the PM system, the concentration of the plated compounds is proprietary and not available to the public. This lack of MIC information was the major stumbling block in implementing this system. However, using the method of calculation presented here it is possible to achieve meaningful clustering without invoking synergy or antagonism.

This study has also demonstrated a minimum number of points for composition of a comparative database. It is likely that clustering results would improve with a larger database sample number, and perhaps even resolve the ambiguity surrounding the assignment of unique MOA. While our future efforts will be on populating this database with non-commercial antimicrobials directed at compounds 6628 and 6021, the public availability of the database (Supporting Material Table 2) from this work will hopefully spur more analyses into PM assignment of MOA.

Supplementary Material

Refer to Web version on PubMed Central for supplementary material.

Acknowledgments

This work was supported by an IDIQ contract (HHSN2662004000041) from the NIH NIAID Division of Microbiology and Infectious Disease, and by the Sitlington Chair in Infectious Diseases (both to WWB). We thank Drs. Darrell Berlin and Richard Bunce (Oklahoma State Univeristy Department of Chemistry) for synthesis of RAB1 through funding from NIH NIAID R01-AI-090685 (to WWB). We are appreciative for the support of lab members including Esther Barrow, Phil Bourne, Patricia Clinkenbeard and Mary Henry.

REFERENCES

Bailey AM, Paulsen IT, et al. RamA confers multidrug resistance in Salmonella enterica via increased expression of acrB, which is inhibited by chlorpromazine. Antimicrobial agents and chemotherapy. 2008; 52(10):3604–3611. [PubMed: 18694955]

Baker M. Academic screening goes high-throughput. Nature Methods. 2010; 7(10):787–792.

Barrow, EW.; Bourne, PC., et al. American Society for Microbiology Biodefense and Emerging Diseases Research Meeting. Washington DC: ASM; 2007. MIC and FIC Evaluations of Select Agents Using High-throughput Screening, Abstract 072 (D).

Barrow EW, Dreier J, et al. In Vitro Efficacy of New Antifolates against Trimethoprim-Resistant Bacillus anthracis. Antimicrob Agents Chemother. 2007; 51(12):4447–4452. [PubMed: 17875993]

Biolog. Identifying Antimicrobials and Their Mechanism of Action Using Phenotype Microarrays; Guiding Structure Activity Relationship (SAR) Analysis Using Phenotype Microarrays. (Application Notes).

Bochner, B. Phenotype Microarrays: Their Use in Antibiotic Discovery. In: Dougherty, TJ.; Projan, SJ., editors. Microbial Genomics and Drug Discovery. Marcel Dekker, Inc; 2003. p. 135-146.

Bochner BR, Siri M, et al. Assay of the multiple energy-producing pathways of mammalian cells. PloS one. 2011; 6(3):e18147. [PubMed: 21455318]

Bourne CR, Barrow EW, et al. Inhibition of antibiotic-resistant Staphylococcus aureus by the broad-spectrum dihydrofolate reductase inhibitor RAB1. Antimicrobial agents and chemotherapy. 2010; 54(9):3825–3833. [PubMed: 20606069]

Bourne CR, Bunce RA, et al. Crystal structure of Bacillus anthracis dihydrofolate reductase with the dihydrophthalazine-based trimethoprim derivative RAB1 provides a structural explanation of potency and selectivity. Antimicrob Agents Chemother. 2009; 53(7):3065–3073. [PubMed: 19364848]

Braden B. The Surveyor's Area Formula. The College Mathematics Journal. 1986; 17(4):326–337.

Brazas MD, Hancock RE. Using microarray gene signatures to elucidate mechanisms of antibiotic action and resistance. Drug discovery today. 2005; 10(18):1245–1252. [PubMed: 16213417]

Brunton, LL.; Chabner, BA., et al. Therapeutics. McGraw-Hill Companies; 2011. Goodman & Gilman's The Pharmacological Basis of.

Cheong CG, Wolan DW, et al. Crystal structures of human bifunctional enzyme aminoimidazole-4-carboxamide ribonucleotide transformylase/IMP cyclohydrolase in complex with potent sulfonyl-containing antifolates. The Journal of biological chemistry. 2004; 279(17):18034–18045. [PubMed: 14966129]

Chidley C, Haruki H, et al. A yeast-based screen reveals that sulfasalazine inhibits tetrahydrobiopterin biosynthesis. Nature chemical biology. 2011; 7(6):375–383.

Chou TC. Drug combination studies and their synergy quantification using the Chou-Talalay method. Cancer research. 2010; 70(2):440–446. [PubMed: 20068163]

CLSI. Methods for dilution antimicrobial susceptibility tests for bacteria that grow aerobically; approved standard 8th edition. 2009; 29(2):1–65.

CLSI. Performance Standards for Antimicrobial Susceptibility Testing. 2010; 29(3):1–153.

dela Cruz TE, Schulz BE, et al. Carbon source utilization by the marine Dendryphiella species D. arenaria and D. salina. FEMS microbiology ecology. 2006; 58(3):343–353. [PubMed: 17117979]

Edwards RL, Dalebroux ZD, et al. Legionella pneumophila couples fatty acid flux to microbial differentiation and virulence. Molecular microbiology. 2009; 71(5):1190–1204. [PubMed: 19170883]

Fabich AJ, Leatham MP, et al. Genotype and phenotypes of an intestine-adapted Escherichia coli K-12 mutant selected by animal passage for superior colonization. Infection and immunity. 2011; 79(6): 2430–2439. [PubMed: 21422176]

Fulmer T. Rethinking mechanisms of drug discovery. Science-Business eXchange. 2011; 4(27):1–3.

Gaulton A, Bellis LJ, et al. ChEMBL: a large-scale bioactivity database for drug discovery. Nucleic acids research. 2011

Grim SA, Rapp RP, et al. Trimethoprim-sulfamethoxazole as a viable treatment option for infections caused by methicillin-resistant Staphylococcus aureus. Pharmacotherapy. 2005; 25(2):253–264. [PubMed: 15767239]

Ho SW, Jung D, et al. Effect of divalent cations on the structure of the antibiotic daptomycin. European biophysics journal. 2008; 37(4):421–433. [PubMed: 17968536]

Kawai M, BaMaung NY, et al. Development of sulfonamide compounds as potent methionine aminopeptidase type II inhibitors with antiproliferative properties. Bioorganic & medicinal chemistry letters. 2006; 16(13):3574–3577. [PubMed: 16632353]

Li C, Xu L, et al. Virtual screening of human 5-aminoimidazole-4-carboxamide ribonucleotide transformylase against the NCI diversity set by use of AutoDock to identify novel nonfolate inhibitors. Journal of medicinal chemistry. 2004; 47(27):6681–6690. [PubMed: 15615517]

Li X, Zolli-Juran M, et al. Multicopy suppressors for novel antibacterial compounds reveal targets and drug efflux susceptibility. Chemistry & biology. 2004; 11(10):1423–1430. [PubMed: 15489169]

Loh KD, Gyaneshwar P, et al. A previously undescribed pathway for pyrimidine catabolism. Proceedings of the National Academy of Sciences of the United States of America. 2006; 103(13): 5114–5119. [PubMed: 16540542]

Lorian, V., editor. Antibiotics in Laboratory Medicine. New York: Lipincott Williams and Wilkins; 1996.

Mesak LR, Davies J. Phenotypic changes in ciprofloxacin-resistant Staphylococcus aureus. Research in microbiology. 2009; 160(10):785–791. [PubMed: 19818400]

Miller AA, Bundy GL, et al. Discovery and characterization of QPT-1, the progenitor of a new class of bacterial topoisomerase inhibitors. Antimicrobial agents and chemotherapy. 2008; 52(8):2806–2812. [PubMed: 18519725]

Mills SD. When will the genomics investment pay off for antibacterial discovery? Biochemical pharmacology. 2006; 71(7):1096–1102. [PubMed: 16387281]

Nagy V, Seidl V, et al. Application of DNA bar codes for screening of industrially important fungi: the haplotype of Trichoderma harzianum sensu stricto indicates superior chitinase formation. Applied and environmental microbiology. 2007; 73(21):7048–7058. [PubMed: 17827332]

Namba K, Zheng X, et al. Design and synthesis of benzenesulfonanilides active against methicillin-resistant Staphylococcus aureus and vancomycin-resistant Enterococcus. Bioorganic & medicinal chemistry. 2008; 16(11):6131–6144. [PubMed: 18468909]

National (Center for Biotechnology Information AID=365). PubChem BioAssay Database. Source=National Cancer Institute Molecular Targets Library.

National (Center for Biotechnology Information AID=366). PubChem BioAssay Database. Source=National Cancer Institute Molecular Targets Library.

National (Center for Biotechnology Information AID=372). PubChem BioAssay Database. Source=National Cancer Institute Molecular Targets Library.

Payne DJ, Gwynn MN, et al. Drugs for bad bugs: confronting the challenges of antibacterial discovery. Nature reviews. 2007; 6(1):29–40.

Peifer M, Weiss J, et al. Analysis of compound synergy in high-throughput cellular screens by population-based lifetime modeling. PloS one. 2010; 5(1):e8919. [PubMed: 20111714]

Pietiainen M, Francois P, et al. Transcriptome analysis of the responses of Staphylococcus aureus to antimicrobial peptides and characterization of the roles of vraDE and vraSR in antimicrobial resistance. BMC genomics. 2009; 10:429. [PubMed: 19751498]

Plouffe D, Brinker A, et al. In silico activity profiling reveals the mechanism of action of antimalarials discovered in a high-throughput screen. Proceedings of the National Academy of Sciences of the United States of America. 2008; 105(26):9059–9064. [PubMed: 18579783]

Robbel L, Marahiel MA. Daptomycin, a bacterial lipopeptide synthesized by a nonribosomal machinery. The Journal of biological chemistry. 2010; 285(36):27501–27508. [PubMed: 20522545]

Sabet S, Diallo L, et al. Characterization of halophiles isolated from solar salterns in Baja California, Mexico. Extremophiles. 2009; 13(4):643–656. [PubMed: 19418017]

Sauer JD, Bachman MA, et al. The phagosomal transporter A couples threonine acquisition to differentiation and replication of Legionella pneumophila in macrophages. Proceedings of the National Academy of Sciences of the United States of America. 2005; 102(28):9924–9929. [PubMed: 15998735]

Seidl V, Druzhinina IS, et al. A screening system for carbon sources enhancing beta-N-acetylglucosaminidase formation in Hypocrea atroviridis (Trichoderma atroviride). Microbiology (Reading, England). 2006; 152(7):2003–2012.

Skold O. Sulfonamide resistance: mechanisms and trends. Drug Resist Update. 2000; 3(3):155–160.

Stirrett KL, Ferreras JA, et al. A multicopy suppressor screening approach as a means to identify antibiotic resistance determinant candidates in Yersinia pestis. BMC microbiology. 2008; 8:122. [PubMed: 18644132]

Tadokoro T, Kanaya S. Ribonuclease H: molecular diversities, substrate binding domains, and catalytic mechanism of the prokaryotic enzymes. The FEBS journal. 2009; 276(6):1482–1493. [PubMed: 19228197]

Tohsato Y, Mori H. Phenotype profiling of single gene deletion mutants of E. coli using Biolog technology. Genome informatics. 2008; 21:42–52. [PubMed: 19425146]

Tracy BS, Edwards KK, et al. Carbon and nitrogen substrate utilization by archival Salmonella typhimurium LT2 cells. BMC evolutionary biology. 2002; 2:14. [PubMed: 12217081]

Tremaroli V, Workentine ML, et al. Metabolomic investigation of the bacterial response to a metal challenge. Applied and environmental microbiology. 2009; 75(3):719–728. [PubMed: 19047385]

Valderas MW, Andi B, et al. Examination of intrinsic sulfonamide resistance in Bacillus anthracis: A novel assay for dihydropteroate synthase. Biochim Biophys Acta. 2008

von Eiff C, McNamara P, et al. Phenotype microarray profiling of Staphylococcus aureus menD and hemB mutants with the small-colony-variant phenotype. Journal of bacteriology. 2006; 188(2): 687–693. [PubMed: 16385058]

Wang H, Claveau D, et al. High-frequency transposition for determining antibacterial mode of action. Nature chemical biology. 2011; 7(10):720–729.

Wiater, LA.; Madejska, E., et al. Grouping Antimicrobials by their Mechanism of Growth Inhibition using Arrays of Synergy and Antagonism Values; International Conference on Antimicrobial Agents and Chemotherapy; Chicago, IL. 2007.

Xu HH, Trawick JD, et al. Staphylococcus aureus TargetArray: comprehensive differential essential gene expression as a mechanistic tool to profile antibacterials. Antimicrobial agents and chemotherapy. 2010; 54(9):3659–3670. [PubMed: 20547796]

Xu L, Li C, et al. Crystal structure of avian aminoimidazole-4-carboxamide ribonucleotide transformylase in complex with a novel non-folate inhibitor identified by virtual ligand screening. The Journal of biological chemistry. 2004; 279(48):50555–50565. [PubMed: 15355974]

Yocum RR, Rasmussen JR, et al. The mechanism of action of penicillin. Penicillin acylates the active site of Bacillus stearothermophilus D-alanine carboxypeptidase. The Journal of biological chemistry. 1980; 255(9):3977–3986. [PubMed: 7372662]

Zhang J, Biswas I. A phenotypic microarray analysis of a Streptococcus mutans liaS mutant. Microbiology (Reading, England). 2009; 155(1):61–68.

Zhang XX, Rainey PB. Dual involvement of CbrAB and NtrBC in the regulation of histidine utilization in Pseudomonas fluorescens SBW25. Genetics. 2008; 178(1):185–195. [PubMed: 18202367]

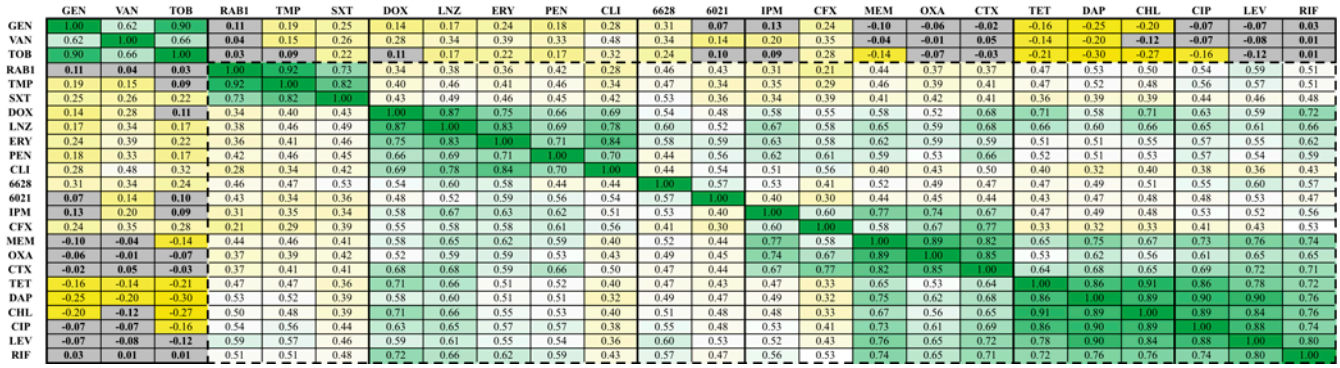

	GEN	VAN	TOB	RAB1	TMP	SXT	DOX	LNZ	ERY	PEN	CLI	6628	6021	IPM	CFX	MEM	OXA	CTX	TET	DAP	CHL	CIP	LEV	RIF
GEN	1.00	0.62	0.90	0.11	0.19	0.25	0.14	0.17	0.24	0.18	0.28	0.31	0.07	0.13	0.24	-0.10	-0.06	-0.02	-0.16	-0.25	-0.20	-0.07	-0.07	0.03
VAN	0.62	1.00	0.66	0.04	0.15	0.26	0.28	0.34	0.39	0.33	0.48	0.34	0.14	0.20	0.35	-0.04	-0.01	0.05	-0.14	-0.20	-0.12	-0.07	-0.08	0.01
TOB	0.90	0.66	1.00	0.03	0.09	0.22	0.11	0.17	0.22	0.17	0.32	0.24	0.10	0.09	0.28	-0.14	-0.07	-0.03	-0.21	-0.30	-0.27	-0.16	-0.12	0.01
RAB1	0.11	0.04	0.03	1.00	0.92	0.73	0.34	0.38	0.36	0.42	0.28	0.46	0.43	0.31	0.21	0.44	0.37	0.37	0.47	0.53	0.50	0.54	0.59	0.51
TMP	0.19	0.15	0.09	0.92	1.00	0.82	0.40	0.46	0.41	0.46	0.34	0.47	0.34	0.35	0.29	0.46	0.39	0.41	0.47	0.52	0.48	0.56	0.57	0.51
SXT	0.25	0.26	0.22	0.73	0.82	1.00	0.43	0.49	0.46	0.45	0.42	0.53	0.36	0.34	0.39	0.41	0.42	0.41	0.36	0.39	0.39	0.44	0.46	0.48
DOX	0.14	0.28	0.11	0.34	0.40	0.43	1.00	0.87	0.75	0.66	0.69	0.54	0.48	0.58	0.55	0.58	0.52	0.68	0.71	0.58	0.71	0.63	0.59	0.72
LNZ	0.17	0.34	0.17	0.38	0.46	0.49	0.87	1.00	0.83	0.69	0.78	0.60	0.52	0.67	0.58	0.65	0.59	0.68	0.66	0.60	0.66	0.65	0.61	0.66
ERY	0.24	0.39	0.22	0.36	0.41	0.46	0.75	0.83	1.00	0.71	0.84	0.58	0.59	0.63	0.58	0.62	0.59	0.59	0.51	0.51	0.55	0.57	0.55	0.62
PEN	0.18	0.33	0.17	0.42	0.46	0.45	0.66	0.69	0.71	1.00	0.70	0.44	0.56	0.62	0.61	0.59	0.53	0.66	0.52	0.51	0.53	0.57	0.54	0.59
CLI	0.28	0.48	0.32	0.28	0.34	0.42	0.69	0.78	0.84	0.70	1.00	0.44	0.54	0.51	0.56	0.40	0.43	0.50	0.40	0.32	0.40	0.38	0.36	0.43
6628	0.31	0.34	0.24	0.46	0.47	0.53	0.54	0.60	0.58	0.44	0.44	1.00	0.57	0.53	0.41	0.52	0.49	0.47	0.47	0.49	0.51	0.55	0.60	0.57
6021	0.07	0.14	0.10	0.43	0.34	0.36	0.48	0.52	0.59	0.56	0.54	0.57	1.00	0.40	0.30	0.44	0.45	0.44	0.43	0.47	0.48	0.48	0.53	0.47
IPM	0.13	0.20	0.09	0.31	0.35	0.34	0.58	0.67	0.63	0.62	0.51	0.53	0.40	1.00	0.60	0.77	0.74	0.67	0.47	0.49	0.48	0.53	0.52	0.56
CFX	0.24	0.35	0.28	0.21	0.29	0.39	0.55	0.58	0.58	0.61	0.56	0.41	0.30	0.60	1.00	0.58	0.67	0.77	0.33	0.32	0.33	0.41	0.43	0.53
MEM	-0.10	-0.04	-0.14	0.44	0.46	0.41	0.58	0.65	0.62	0.59	0.40	0.52	0.44	0.77	0.58	1.00	0.89	0.82	0.65	0.75	0.67	0.73	0.76	0.74
OXA	-0.06	-0.01	-0.07	0.37	0.39	0.42	0.52	0.59	0.59	0.53	0.43	0.49	0.45	0.74	0.67	0.89	1.00	0.85	0.53	0.62	0.56	0.61	0.65	0.65
CTX	-0.02	0.05	-0.03	0.37	0.41	0.41	0.68	0.68	0.59	0.66	0.50	0.47	0.44	0.67	0.77	0.82	0.85	1.00	0.64	0.68	0.65	0.69	0.72	0.71
TET	-0.16	-0.14	-0.21	0.47	0.47	0.36	0.71	0.66	0.51	0.52	0.40	0.47	0.43	0.47	0.33	0.65	0.53	0.64	1.00	0.86	0.91	0.86	0.78	0.72
DAP	-0.25	-0.20	-0.30	0.53	0.52	0.39	0.58	0.60	0.51	0.51	0.32	0.49	0.47	0.49	0.32	0.75	0.62	0.68	0.86	1.00	0.89	0.90	0.90	0.76
CHL	-0.20	-0.12	-0.27	0.50	0.48	0.39	0.71	0.66	0.55	0.53	0.40	0.51	0.48	0.48	0.33	0.67	0.56	0.65	0.91	0.89	1.00	0.89	0.84	0.76
CIP	-0.07	-0.07	-0.16	0.54	0.56	0.44	0.63	0.65	0.57	0.57	0.38	0.55	0.48	0.53	0.41	0.73	0.61	0.69	0.86	0.90	0.89	1.00	0.88	0.74
LEV	-0.07	-0.08	-0.12	0.59	0.57	0.46	0.59	0.61	0.55	0.54	0.36	0.60	0.53	0.52	0.43	0.76	0.65	0.72	0.78	0.90	0.84	0.88	1.00	0.80
RIF	0.03	0.01	0.01	0.51	0.51	0.48	0.72	0.66	0.62	0.59	0.43	0.57	0.47	0.56	0.53	0.74	0.65	0.71	0.72	0.76	0.76	0.74	0.80	1.00

Figure 1.

Pearson correlation values between antimicrobials and test compounds. Values approach 1 (shaded green) as the agreement between data sets increases. Boxes shaded gray were excluded from analysis due to $p > 0.05$; shading is from lowest (yellow) to highest (green) values.

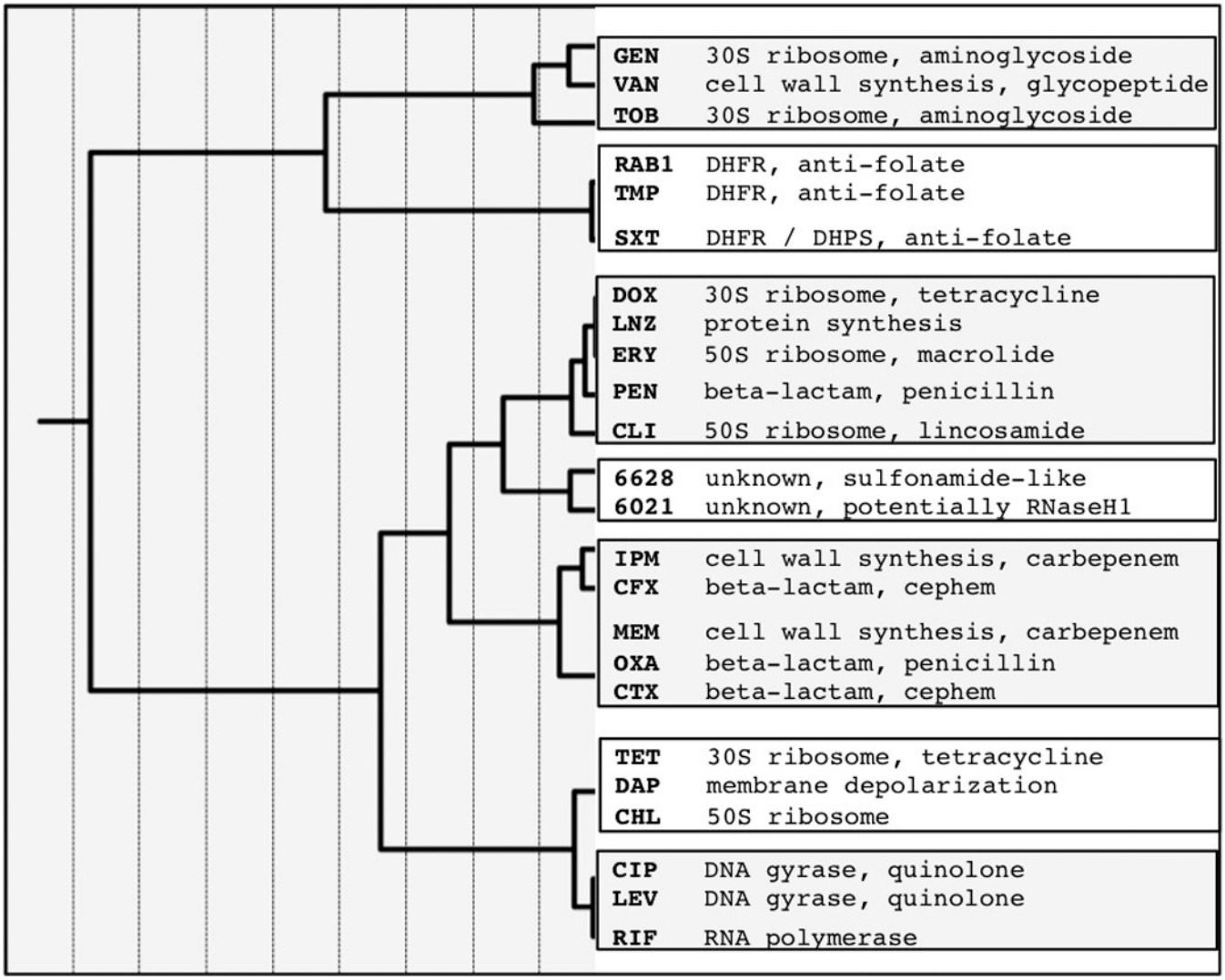

Figure 2.
Dendrogram of MOA clusters derived from PM assays. Compound abbreviations are given in the Materials and Methods section.

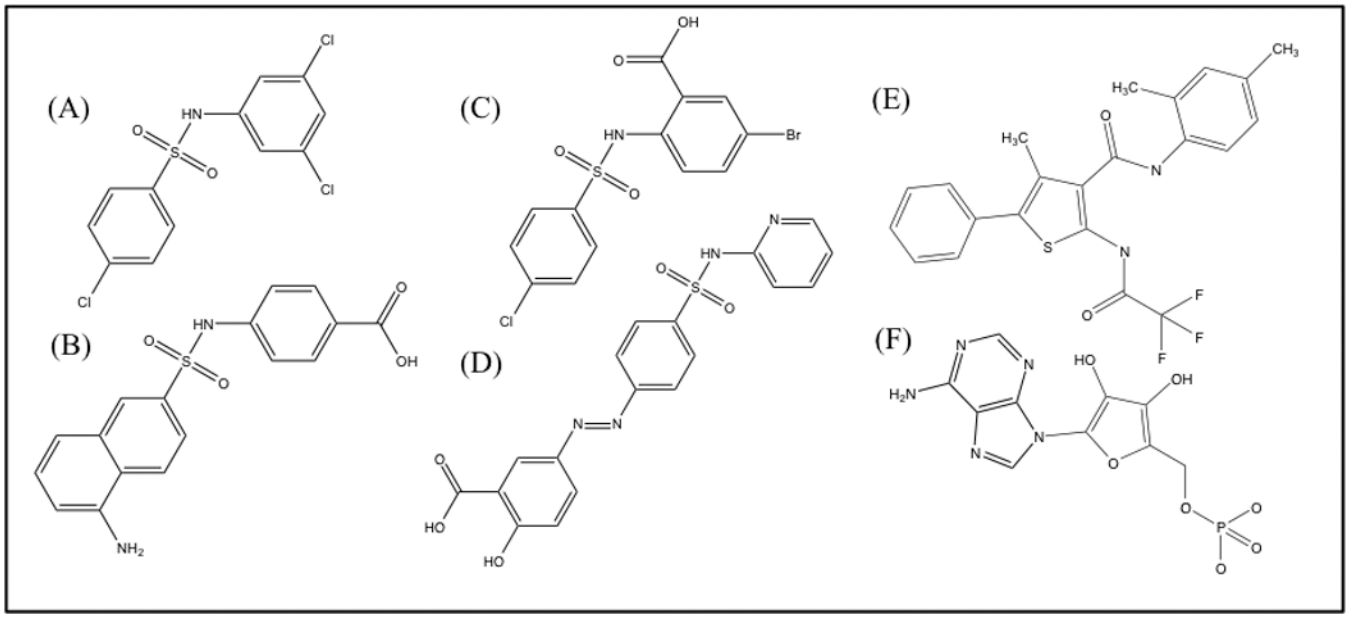

Figure 3.

Tested compounds with unknown MOA and structurally similar compounds identified in the literature. (A) Compound 6628, a benzene sulfonamide. (B) An inhibitor of human 5-aminoimidazole-4-carboxamide ribonucleotide transformylase (Li et al., 2004a). (C) An inhibitor of human methionine aminopeptidase type II (Kawai et al., 2006). (D) An inhibitor of human sepiapterin reductase (Chidley et al., 2011). (E) Compound 6021, a thiophene carboxamide. (F) An adenine ribonucleotide.

Table 1

Minimum inhibitory concentration (MIC) for 21 antimicrobials and three test compounds used in the Phenotype Microarray assay. CLSI values reported in (2010) "Performance Standards for Antimicrobial Susceptibility Testing.", and repeated in-house using the same testing methods, incubated at 37 °C for 18–20 hours. NA indicates no CLSI MIC value available. Biolog MIC determinations were carried out using Biolog reagents and plates, at 33 °C for 24 hours. Compound abbreviations are given in the Materials and Methods section.

Target	Class	abbreviation	CLSI reported MIC (μg/mL)	CLSI method in-house MIC (μg/mL)	Biolog reagents in-house MIC (μg/mL)
30S ribosome	**aminoglycoside**	GEN	0.12 – 1	0.25 – 0.5	2
		TOB	0.12 – 1	0.25 – 0.5	2
	tetracycline	DOX	0.12 – 0.5	0.125 – 0.25	0.25
		TET	0.12 – 1	0.25 – 0.5	0.25
50S ribosome	**lincosamide**	CLI	0.06 – 0.25	0.0625 – 0.125	0.125
	macrolide	ERY	0.25 – 1	0.25 – 1	2
50S ribosome	**no class assigned**	CHL	2 – 16	4 – 8	16
protein synthesis	**no class assigned**	LNZ	1 – 4	1 – 2	2
cell wall synthesis	**carbepenem**	IPM	0.015 – 0.06	0.008 – 0.016	0.03125
		MEM	0.03 – 0.1	0.03 – 0.25	0.0625
beta-lactam	**cephalosporin**	CTX	1 – 4	1 – 2	1
		CFX	0.5 – 2	1	1
	penicillin	OXA	0.12 – 0.5	0.0625 – 0.125	0.25
		PEN	0.25 – 2	1	32
peptidoglycan synthesis	**glycopeptide**	VAN	0.5 – 2	1	2
DNA gyrase/topoisomerase	**quinolone**	CIP	0.12 – 0.5	0.25	0.5
		LEV	0.06 – 0.5	0.0625 – 0.125	0.25
DHFR/DHPS	**anti-folate**	TMP	1 – 4	2 – 4	1
		SXT	≤ 0.5/9.5	0.05/0.095	0.05/0.095
RNA polymerase	**no class assigned**	RIF	0.004 – 0.015	0.02 – 0.004	0.004

Target	Class	abbreviation	CLSI reported MIC (μg/mL)	CLSI method in-house MIC (μg/mL)	Biolog reagents in-house MIC (μg/mL)
membrane depolarization	Lipopeptide	DAP	0.12 – 1	1 – 4	50
DHFR	Test compound	RAB1	NA	0.06 – 0.25	0.015 – 0.03
putative DHPS	Test compound	6628	NA	4 – 8	2
putative RNaseH1	Test compound	6021	NA	≤ 1 – 2	> 32